



Exploring the Use of Iterative Recordings of Frequency-Following Responses to Uncover Hidden Hearing Loss

DOI:
[10.3813/AAA.919257](https://doi.org/10.3813/AAA.919257)

[Link to publication record in Manchester Research Explorer](#)

Citation for published version (APA):

Marmel, F., Perugia, E., & Kluk-De Kort, K. (2018). Exploring the Use of Iterative Recordings of Frequency-Following Responses to Uncover Hidden Hearing Loss. *Acta Acustica united with Acustica*, 104(5), 878-882. <https://doi.org/10.3813/AAA.919257>

Published in:

Acta Acustica united with Acustica

Citing this paper

Please note that where the full-text provided on Manchester Research Explorer is the Author Accepted Manuscript or Proof version this may differ from the final Published version. If citing, it is advised that you check and use the publisher's definitive version.

General rights

Copyright and moral rights for the publications made accessible in the Research Explorer are retained by the authors and/or other copyright owners and it is a condition of accessing publications that users recognise and abide by the legal requirements associated with these rights.

Takedown policy

If you believe that this document breaches copyright please refer to the University of Manchester's Takedown Procedures [<http://man.ac.uk/04Y6Bo>] or contact openresearch@manchester.ac.uk providing relevant details, so we can investigate your claim.



Exploring the Use of Iterative Recordings of Frequency-Following Responses to Uncover Hidden Hearing Loss

Frederic Marmel, Emanuele Perugia, Karolina Kluk

Manchester Centre for Audiology and Deafness, University of Manchester, Manchester Academic Health Science Centre, M13 9PL, UK. frederic.marmel@gmail.com

Summary

Hidden hearing loss may be related to a loss or a dysfunction of auditory nerve fibres associated with noise exposure history and aging. Such functional degradation should reduce the stimulus information encoded in the auditory nerve, but information pooling across fibres may result in frequency-following responses (FFRs) being barely different from normal responses. This study investigated the possibility of amplifying the reduction of stimulus information by recording the FFR iteratively; i.e. by converting the FFR to a stimulus file and recording another FFR in response to it. Iterated FFRs were found to contain detectable stimulus information, but there was no evidence that they reflected hidden hearing loss.

© 2018 The Author(s). Published by S. Hirzel Verlag · EAA. This is an open access article under the terms of the Creative Commons Attribution (CC BY 4.0) license (<https://creativecommons.org/licenses/by/4.0/>).

PACS no. 43.64.Ri, 43.66.Sr, 43.64.Wn

1. Introduction

Hidden hearing loss (HHL) has been a hot topic for a few years (see [1, 2] for reviews) due to: i) the long-known puzzling fact that audiometric thresholds do not always reflect listeners difficulties hearing speech in noise (the HHL phenotype) and ii) recent studies in rodents showing that alterations to primary auditory synapses and nerve fibers (cochlear synaptopathy) can predate the degeneration of sensory cells. These studies led to the proposal that cochlear synaptopathy and preserved inner hair cells might hence serve as physiological substrates of HHL [3].

Human studies seeking to uncover HHL have focused on listeners with significant lifetime noise exposure and/or listeners suffering from tinnitus, and have looked for evidence of cochlear synaptopathy in the form of correlations between early auditory electroencephalographic (EEG) responses, lifetime noise exposure, and supra-threshold hearing performance. This approach has struggled to uncover HHL [8, 9, 10], maybe partly because of a lack of sensitivity of the EEG measures. This study aimed to propose a novel FFR recording paradigm that might be more sensitive to small AN alterations and thereby facilitate the uncovering of HHL.

2. Rationale and hypotheses

2.1. Hidden hearing loss should be associated with degraded neural representations of short-duration acoustic features

HHL might be a consequence of the stochastic nature of action potentials combined with cochlear synaptopathy resulting in fewer functional auditory nerve fibers (ANFs) [11, 12]. The quantity of stimulus information conveyed by an individual ANF depends (i) on its instantaneous probability of firing as a function of stimulus intensity, and (ii) on the stimulus duration. An ANF's probability of firing increases with increasing sound pressure up to its saturation level, hence a non-saturated ANF is more likely to convey high-intensity than low-intensity sound features. Also, action potentials occur at random along the duration of a fixed-level stimulus (stochastic firing). Hence, in the hypothetical absence of non-linear transient effects like adaptation (which enhances the probability of firing at the stimulus onset [13]) or refractoriness, a long sustained stimulus is more likely to evoke an action potential in an individual ANF than a shorter stimulus of the same intensity [14]. In short, stochastic firing suggests that individual ANFs provide incomplete representations of the stimulus features with low-intensity and transient features being less likely to be represented in their spike trains than high-intensity and long features. In a healthy auditory nerve, a high-quality neural representation of sound would be granted by the pooling of the spike trains from all available ANFs. However, in case of cochlear synaptopathy, the

Received 21 March 2018,
accepted 20 September 2018.

comparatively fewer surviving ANFs might be insufficient to compensate for the limited information encoding by individual ANFs of soft and short acoustic features.

The reasoning of [11, 12] was tested experimentally in [11] using stochastically undersampled stimuli, i.e. vocoded stimuli that were degraded by stochastic samplers in order to simulate the perceptual effect of a reduction of the number of ANFs. Reducing the number of samplers impaired speech recognition in noise but not in quiet, and left detection thresholds for 100-ms pure tones within the normal range, consistent with the HHL phenotype. In a later study [13], reducing the number of stochastic samplers resulted in an elevation of detection threshold for short durations but not for long durations. Finally, reducing the number of ANFs in a physiological model of the auditory periphery (the MAP model, [16]) resulted in elevated simulated detection thresholds for short durations but not for long durations (unpublished). These results are consistent with the reasoning in [11] that cochlear synaptopathy should result in degraded encoding of short acoustic features.

2.2. Iterative FFRs might reveal degraded neural representations of short-duration acoustic features

We reasoned that it might be possible to detect HHL objectively using EEG responses to short transient acoustic features such as to individual pulses in a pulse train. The FFR reflects stimulus-related periodicities and mimics the stimulus waveform in normal-hearing listeners faithfully, to the point that FFRs to words can be heard as intelligible speech when converted from neural to audio signal. Pulse trains with a periodicity of 100–200 Hz evoke strong FFRs in normal-hearing listeners [17] and we expect that the representation of pulses in the FFR might be degraded if a listener's encoding of short acoustic features was impaired by cochlear synaptopathy. Moreover, it might be possible to use the fact that FFRs can be 'sonified' [18] to amplify the effect of small amounts of cochlear synaptopathy by recording successive FFRs iteratively; that is by using a first recorded FFR as an audio stimulus to record a second FFR, and repeating this process. Pulse trains should be less and less well represented in the FFRs as the number of iterations increases, as the effects of the neural coding alterations on the encoding of the pulse trains would pile up. Thanks to this acceleration of degraded neural encoding, iterated FFRs could be a measure of auditory nerve fibers alterations more sensitive and less susceptible to between- and within-participants variability than a single FFR recording. Figure 1A illustrates this rationale with the stochastic undersampling vocoder of [11, 12, 13].

We measured FFRs in listeners with a wide range of age and lifetime noise exposure. We also collected behavioral measures: absolute pure-tone thresholds for high frequencies (> 8 kHz) and detection thresholds elevation for short vs. long tones (temporal integration). It has been proposed that both these measures should be elevated when there is

cochlear synaptopathy ([8, 12, 19] for the former, [15] for the latter).

We hypothesized that the neural representation of the original pulse train stimulus would be weaker in the iterated FFRs than in the first FFR, and that this representation would show stronger correlations with the behavioral measures potentially linked to HHL for the iterated FFRs than for the first FFR.

3. Methods

3.1. FFRs collection and processing

The EEG was recorded with BioSemi ActiveTwo System (BioSemi B.V., Amsterdam, Netherlands) at a sampling rate of 16384 Hz from five central electrodes (FC1, FC2, Cz, CP1, and CP2) and the two earlobes. Participants relaxed in a reclined position. FFRs were first recorded in response to 2100 repetitions of a periodic pulse train (pulse rate = 128 Hz). The FFRs were processed (see below) and the average FFR (henceforth referred to as FFR1) was replicated 2100 times and converted to audio to obtain a second set of recordings. This second set of FFRs was processed, and the average FFR (referred to as FFR2) was replicated 2100 times and converted to audio to obtain a third set of FFRs (whose average will be referred to as FFR3). All stimuli were generated digitally in MATLAB (The Mathworks, USA) and presented binaurally through E•A•RTONE 3A insert earphones (10 Ohm, Aearo Technologies, USA) shielded in Mu-metal. The presentation level was 80 dB SPL, except for two participants who found it too loud (the level was then set to 77 dB SPL). Figure 1B shows the FFRs of one example participant (P13).

3.2. FFR1 processing and generation of FFR2-3

For each recording, the EEG was referenced to the average of the two earlobe electrodes and bandpass-filtered between 60–3000 Hz. Epochs corresponding to the last 2000 pulse train repetitions were extracted and baseline-corrected. As the onset delay of an FFR is typically 8–9 ms, FFR2 should be delayed by ~8–9 ms compared to FFR1, as should be FFR3 compared to FFR2. The baseline windows were shifted accordingly: FFR1 processing used the last 40 ms of each epoch, FFR2 processing used the first 10 ms and the last 30 ms, and FFR3 processing used the first 20 ms and the last 20 ms. For each recording, the epochs were then sorted according to their maximum absolute amplitude and the top 10% were assumed to not be artifact-free and were discarded. This resulted in the same number of 'clean' epochs for every FFR across iterations and participants. The 1800 'clean' epochs were averaged, and the averages – obtained for the five electrodes – were averaged together, giving FFR1, 2, or 3. For conversion to audio, the FFRs were centered on zero and had 8-ms cosine-squared onset and offset ramps added.

Each recording session started with a control condition: the EEG was recorded as for FFR1 but the participant's

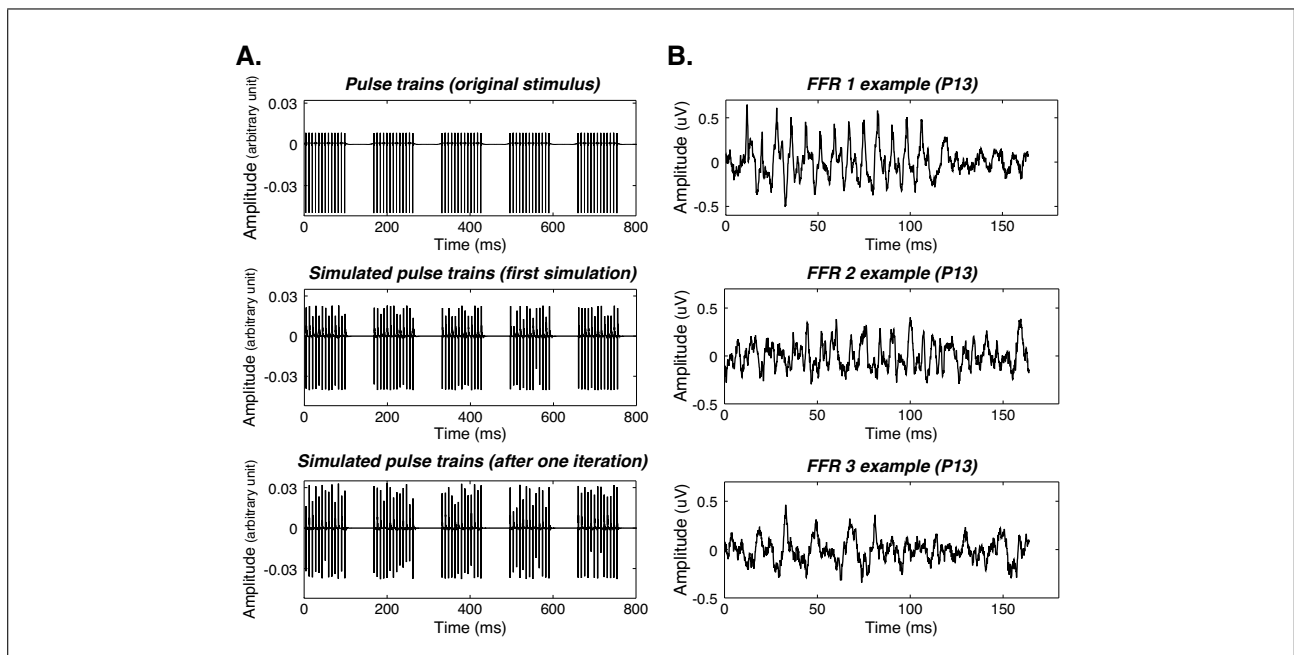


Figure 1. Stochastically undersampled pulse trains (A) and examples of iterated FFRs (B). (A) Top panel: five repetitions of the pulse train used for the first FFR recordings. Middle panel: The pulse trains were processed with the stochastic undersampling vocoder of [11, 12, 13]. The resulting simulated trains are degraded. Bottom panel: Iterating the process by passing the simulated trains into the vocoder amplified the pulse trains degradation. Amplifying the degradation might be necessary to evidence HHL in clinically normal-hearing listeners who have normal FFRs. (B) Top panel: example of FFR1, elicited by the original pulse train: the 13 pulses are represented clearly. Middle panel: example of FFR2, elicited by the ‘sonified’ FFR1: fewer pulses are visible and they are broader than in FFR1. Bottom panel: example of FFR3: fewer pulses are visible and most of them are broader than in FFR1 and FFR2.

ears were blocked. The average waveform is referred to as FFR0 and reflects the individual noise floor.

3.3. Participants

Thirty-one participants aged between 19 and 58 years old (median = 30 years) were tested. Their audiometric thresholds spanned -2.5 – 16 dB HL in the tested ear (20 left) when averaged between 250 and 8,000 Hz. The tested ear was either the ear with the best audiogram or – if the audiograms were equivalent – the ear with the less variable audiogram. Participants’ lifetime noise exposure was estimated using the NESI (*noise exposure structured interview*) fully described in [8, 9, 19]. Their absolute pure-tone thresholds were measured in the tested ear for 250-ms and 5-ms pure tones with frequencies of 12, 14, and 16 kHz using MultiTheshold (Matlab software described in [20]). Absolute pure-tone thresholds for low frequencies (1, 2, and 4 kHz) were also measured in the same way. Stimuli were presented through circumaural Sennheiser HD650 headphones. The University of Manchesters Research Ethics Committee 1 approved the study.

3.4. Data analysis

The presence of the pulse train stimulus was assessed using the frequency-domain Hotelling’s T^2 (HT2) [21, 22]. For each FFR (including FFR0), fast Fourier transforms (FFT) were computed on each epoch. Then, two-sample HT2 tests were performed to compare FFR1 to 3 to FFR0.

The input features of the HT2s were the real and the imaginary parts of the FFTs for the frequencies of the first seven harmonics of the pulse train frequency (128 Hz). An FFR can contain spectral energy up to ~ 1000 Hz [17]. To quantify how strongly the pulse train was represented in FFR1 to 3 (relative to the control condition FFR0), the T^2 statistics were transformed into the squared Mahalanobis distance, D^2 , which is the multivariate analogue of the d effect size and can be used to describe effects as small ($D^2 = 0.25$), medium ($D^2 = 0.5$), or large ($D^2 > 1$) [23].

To compare the potential sensitivity of FFR1, FFR2 and FFR3 to cochlear synaptopathy, we performed stepwise regression models (with both forward and backward selection, using the computing environment R (R Core Team, [24])). We built models for four dependent variables: age, NESI scores, high-frequency absolute pure-tone thresholds (short and long durations averaged together) and temporal integration (low and high frequencies averaged together). The predictors were automatically selected by the stepwise procedure amongst the D^2 s for FFR1 to 3. Age, NESI scores, and the D^2 s for FFR1 to 3 were log transformed to normalize their distribution.

4. Results

The pulse train was always detectable: D^2 s were significant ($p < 0.05$) for every participant for the three FFRs. However, iterating the FFR reduced the effect size greatly. The median D^2 s were 1.32, 0.13 and 0.08 for FFR1, 2 and

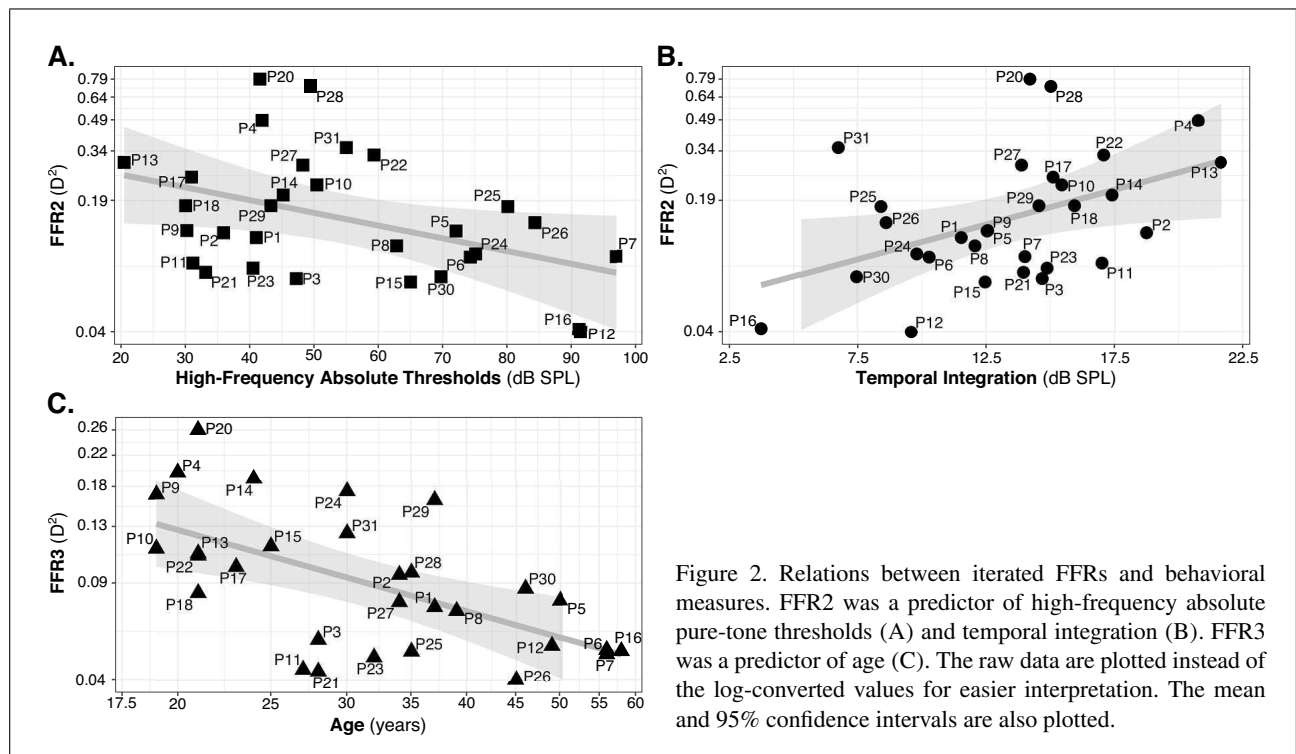


Figure 2. Relations between iterated FFRs and behavioral measures. FFR2 was a predictor of high-frequency absolute pure-tone thresholds (A) and temporal integration (B). FFR3 was a predictor of age (C). The raw data are plotted instead of the log-converted values for easier interpretation. The mean and 95% confidence intervals are also plotted.

3, respectively. One participant (P19) had a D^2 of 24.9 in FFR1 and was removed from the dataset as an outlier. Large D^2 s were only observed for FFR1 ($D^2 > 1$; $n = 19$). Most D^2 s for FFR2 and 3 were trivial, even though they were always statistically significant (< 0.25 ; $n = 23$ for FFR2 and $n = 30$ for FFR3).

Turning to the regression models, the best model for age ($r_{\text{adj}}^2 = 0.35$, $F_{2,27} = 8.95$, $P = 0.0010$) had FFR2 and FFR3 as predictors, but only FFR3 was a significant contributor ($\beta = -0.31$, $T = -2.36$, $P = 0.026$). Greater age was associated with smaller D^2 s in FFR3. The best models for high-frequency absolute pure-tone thresholds ($r_{\text{adj}}^2 = 0.15$, $F_{1,28} = 6.25$, $P = 0.019$) and for temporal integration ($r_{\text{adj}}^2 = 0.17$, $F_{1,28} = 7.14$, $P = 0.012$) only included FFR2 as a predictor (for the absolute pure-tone thresholds: $\beta = -28.21$, $T = -2.50$, $P = 0.019$; for temporal integration: $\beta = 5.74$, $T = -2.67$, $P = 0.012$). Greater high-frequency thresholds were associated with smaller D^2 s in FFR2, but greater temporal integration was associated with larger D^2 s in FFR2. None of the FFR predictors were selected when the NESI scores were the dependent variable. Figure 2 shows the three significant associations.

5. Discussion

This study showed that it is possible to record FFRs in iteration and detect spectral features from the initial stimulus, even after iterating two times. The best regression models included the iterated FFRs but never the first FFR, which suggests that iterated FFRs can be more sensitive to some auditory alterations than a single FFR.

The negative association between iterated FFRs and age is consistent with cochlear synaptopathy following ageing [7]. However, we did not find any association between the FFRs and noise exposure, consistent with the lack of evidence for life-time noise-exposure related synaptopathy in references [8, 9, 19]. The potential importance of including participants with a range of noise exposure broad enough was pointed in [10] when comparing their results to [8]. The NESI scores in the present study ranged from -0.79 to 2.67 , which is a similar spread as in [10], and thus makes it unlikely that the lack of association between the NESI and the FFRs in the present study was due to a limited range of exposure. The positive association between FFR2 and temporal integration was in the opposite direction to the prediction of [15]. In [15], cochlear synaptopathy was predicted to result in steeper temporal integration, whereas shallower temporal integration is usually observed in patients with cochlear (mechanical) hearing loss. Added to the observation that the positive association between FFR2 and high-frequency absolute pure-tone thresholds would be consistent with both cochlear synaptopathy or cochlear mechanical loss, results are overall more consistent with the idea that their cochlear mechanical loss (and not their degree of HHL/synaptopathy) was responsible for the individual differences. However, recalculating the regression models on a subset of 16 participants who had audiometric thresholds at or better than 15 dB HL in both ears did not change the direction of the associations. It might also be the case that the prediction of [15] was wrong: [25] investigated the value of brief-tone audiometry to diagnose cochlear synaptopathy and found brief-tone audiometry to be more consistent with cochlear mechanical loss than with synaptopathy.

In conclusion, recording FFRs iteratively is possible and might provide better sensitivity than a single FFR to some aspects of hearing dysfunction, but there is no evidence that they are sensitive to cochlear synaptopathy and hidden hearing loss.

References

- [1] C. J. Plack, D. Barker, G. Prendergast: Perceptual Consequences of ‘Hidden Hearing Loss. *Trends Hear* **18** (2014).
- [2] C. J. Plack, A. Léger, G. Prendergast, K. Kluk, H. Guest, K. J. Munro: Toward a Diagnostic Test for Hidden Hearing Loss. *Trends Hear* **20** (2016).
- [3] M. Kobel, C. G. Le Prell, J. Liu, J. W. Hawks, J. Bao: Noise-Induced Cochlear Synaptopathy: Past Findings and Future Studies. *Hear Res* **349** (2017) 148–154.
- [4] A. C. Furman, S. G. Kujawa, M. C. Liberman: Noise-Induced Cochlear Neuropathy Is Selective for Fibers with Low Spontaneous Rates. *J Neurophysiol* **110** (2013) 577–586.
- [5] S. G. Kujawa, M. C. Liberman: Adding Insult to Injury: Cochlear Nerve Degeneration after ‘Temporary Noise-Induced Hearing Loss. *J Neurosci* **29** (2009) 14077–85.
- [6] H. W. Lin, A. C. Furman, S. G. Kujawa, M. C. Liberman: Primary Neural Degeneration in the Guinea Pig Cochlea after Reversible Noise-Induced Threshold Shift. *J Assoc Res Otolaryngol* **12** (2011) 605–616.
- [7] Y. Sergeyenko, K. Lall, M. C. Liberman, S. G. Kujawa: Age-Related Cochlear Synaptopathy: An Early-Onset Contributor to Auditory Functional Decline. *J Neurosci* **33** (2013): 13686–94.
- [8] G. Prendergast, H. Guest, K. J. Munro, K. Kluk, A. Léger, D. A. Hall, M. G. Heinz, C. J. Plack: Effects of noise exposure on young adults with normal audiograms I: Electrophysiology. *Hear Res* **344** (2017) 68–81.
- [9] H. Guest, K. J. Munro, G. Prendergast, S. Howe, C. J. Plack: Tinnitus with a normal audiogram: Relation to noise exposure but no evidence for cochlear synaptopathy. *Hear Res* **344** (2017) 265–274.
- [10] J. T. Valderrama, E. F. Beach, I. Yeend, M. Sharma, B. Van Dun, H. Dillon: Effects of lifetime noise exposure on the middle-age human auditory brainstem response, tinnitus and speech-in-noise intelligibility. *Hear Res* **365** (2018) 36–48.
- [11] E. A. Lopez-Poveda, P. Barrios: Perception of stochastically undersampled sound waveforms: a model of auditory deafferentation. *Front Neurosci* **7** (2013).
- [12] E. A. Lopez-Poveda: Why do I hear but not understand? Stochastic undersampling as a model of degraded neural encoding of speech. *Front Neurosci* **8** (2014).
- [13] L. A. Westerman, R. L. Smith: Rapid and short terms adaptation in auditory nerve responses. *Hear Res* **15** (1984).
- [14] P. Heil, H. Neubauer, M. Brown, D. R. F. Irvine: Towards a unifying basis of auditory thresholds: distributions of the first spikes latencies of auditory-nerve fibers. *Hear Res* **238** (2008).
- [15] F. Marmel, M. A. Rodríguez-Mendoza, E. A. Lopez-Poveda: Stochastic undersampling steepens auditory threshold/duration functions: implications for understanding auditory deafferentation and aging. *Front Aging Neurosci* **63** (2015).
- [16] R. Meddis, W. Lecluyse, N. R. Clark, T. Jürgens, C. M. Tan, M. R. Panda, *et al.*: A computer model of the auditory periphery and its application to the study of hearing. *Adv Exp Med Biol* **787** (2013) 11–19.
- [17] G. M. Bidelman: Multichannel recordings of the human brainstem frequency-following response: Scalp topography, source generators, and distinctions from the transient ABR. *Hear Res* **323** (2015) 68–80.
- [18] G. M. Bidelman: Sonification of scalp-recorded frequency-following responses (FFRs) offers improved response detection over conventional statistical metrics. *J Neurosci Methods* **293** (2018) 59–66.
- [19] G. Prendergast, R. E. Millman, H. Guest, K. J. Munro, K. Kluk, R. S. Dewey, D. A. Hall, M. G. Heinz, C. J. Plack: Effects of noise exposure on young adults with normal audiograms II: Behavioral measures. *Hear Res* **356** (2017) 74–86.
- [20] W. Lecluyse, R. Meddis: A simple single-interval adaptive procedure for estimating thresholds in normal and impaired listeners. *J Acoust Soc Am* **126** (2009) 2570–2579.
- [21] J. A. Carballo-Gonzalez, P. Valdes-Sosa, M. Valdes-Sosa: Detection of event related potentials. *Int J Neurosci* **46** (1989) 109–122.
- [22] M. J. Valdes-Sosa, M. A. Bobes, M. C. Perez-Abalo, M. Perera, J. A. Carballo, P. Valdes-Sosa: Comparison of auditory-evoked potential detection methods using signal detection theory. *Audiol Off Organ Int Soc Audiol* **26** (1987) 166–178.
- [23] M. Sapp, F. E. Obiakor, A. J. Gregas, S. Scholze: Mahalanobis distance: A multivariate measure of effect in hypnosis research. *Sleep Hypn* **9** (2007) 67–70.
- [24] R Core Team, 2012. R: a Language and Environment for Statistical Computing. R Foundation for Statistical Computing. Vienna, Austria. ISBN: 3-900051-07-0. Available. <http://www.R-project.org>.
- [25] E. A. López-Poveda, P. T. Johannesen, B. C. Buzo F. Rønne, N. H. Pontoppidan, J. M. Harte: On the value of brief sound audiometry as a diagnostic tool for cochlear synaptopathy. 2017 ARO MidWinter Meeting, 2017.